Selective vibrational pumping of a molecular beam by a stimulated Raman process

Fujio Shimizu
Department of Applied Physics, University of Tokyo, Bunkyo-ku, Tokyo 113, Japan

Kazuko Shimizu and Hiroshi Takuma
Institute for Laser Science and Department of Engineering Physics, University of Electro-Communications, Chofu-shi, Tokyo 182, Japan

(Received 21 November 1984)

Stimulated Raman process is used to selectively pump a highly excited vibrational state in a molecular beam. Theoretical evaluation shows that continuous lasers with power of less than 1 W can efficiently pump a single rotational-vibrational level of many simple molecules. The characteristics of the selectively pumped molecular beam and operational conditions are discussed theoretically. The experiment on a Na_2 beam is found to agree with theoretical predictions. The flux of 4×10^7 s^{-1} in the $v=31$, $J=5$ excited level has been obtained with use of two cw dye lasers with powers of 80 and 300 mW.

I. INTRODUCTION

The laser is a powerful tool for the state-to-state analysis of collision processes in a molecular-beam experiment. A number of studies has been reported on the internal state distribution of molecules after collision using the laser-induced fluorescence technique.[1,2] For the labeling of an internal state of molecules before the collision, only a limited class of states has been investigated. An electronically excited level can be selectively pumped using a tunable visible or near ultraviolet laser.[2–8] The same process labels a ground electronic level by pumping out of its thermal population.[9–14] However, it is rather difficult to label a vibrationally excited level by direct optical transition.[15–22] A transition moment between a highly excited vibrational state and the ground state is prohibitively small. Most coherent infrared sources do not cover a wide enough frequency range which is necessary to pump various excited states from the ground vibrational state. We have demonstrated that a folded two-photon process can be used to selectively pump a vibrationally excited level of a molecular beam.[23–28] This paper describes a detailed theoretical and experimental analysis of our previous report.[27] Folded two-photon pumping via an electronically excited state is applicable for a wide range of molecules, because the selection rule on vibrational transitions $\Delta v=1$ does not apply if the adiabatic potential surfaces of the excited and ground electronic states have different shapes. The tuning requirement of the laser is also eased because of a smaller fractional change of frequency compared to the direct pumping.

A vibrational level may be pumped either by a two-step process or by a stimulated Raman process. In the two-step process, the first laser pumps molecules to an electronically excited intermediate level. Its population is then transferred by the second laser to the vibrationally excited final level by stimulated emission. In a favorable situation, the laser action between the intermediate and final levels may replace the second laser.[28] In the stimulated Raman process neither transition is resonant. The population in the ground state is directly transferred to the final state. Because the intermediate state is off-resonant, the stimulated Raman process is a weaker effect compared to the two-step process in usual circumstances. This does not mean that two-step process is more effective for the selective pumping of a molecular beam. When molecules do not experience collisions, the spontaneous emission plays a crucial role on the pumping efficiency. In the two-step pumping, pumping lasers work towards equalizing the population of relevant three energy levels. If the interaction time of the molecule with lasers is longer than the spontaneous lifetime of the electronically excited state, the population of all three levels decreases through spontaneous decay from the intermediate level to other energy levels. Since the spontaneous decay rate is proportional to the transition probability, this sets an upper limit to the magnitude of the transition moment that can be used for the pumping. The stimulated Raman pumping is free from disturbance by spontaneous emission because the intermediate level is not populated.

Consider a three-level molecule interacting with two lasers as shown in Fig. 1. Laser L_p is nearly resonant to transition $1\rightarrow2$ and L_s to transition $2\rightarrow3$. We can estimate the laser power required for the pumping by the following discussion. To populate level 2 sufficiently, the transition induced by L_p must be saturated,

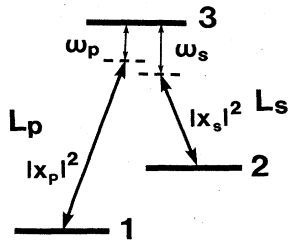

FIG. 1. Energy-level configuration of the folded two-photon pumping.

$$\frac{\mu E}{\hbar}\tau_t \sim 1 , \tag{1}$$

where E is the laser field, μ is the transition moment, and τ_t is the interaction time of the molecule with the lasers. The spontaneous lifetime τ_s of level 2 must be longer than τ_t to avoid depopulation, the former being inversely proportional to the square of the transition moment,

$$\tau_t < \tau_s = \alpha/\mu^2 , \tag{2}$$

where α is a proportionality constant. Therefore, the two-step pumping requires the laser power of

$$E^2 > \hbar/(\alpha\tau_t) . \tag{3}$$

For the stimulated Raman pumping, μ in Eq. (1) is replaced by the effective transition moment $\mu(\mu E/\hbar\omega)$, where ω is the frequency mismatch at the intermediate state. This yields

$$\frac{\mu^2 E^2}{\hbar^2\omega}\tau_t \sim 1 . \tag{4}$$

Equation (4) shows that E^2 is proportional to ω. On the other hand, ω must be large enough so that level 2 is not appreciably populated. The linewidth of the transition $1\rightarrow 2$ is $1/\tau_s$. When $\tau_t \gg \tau_s$, substantial transition occurs even at the far wing of the resonance, because level 2 is repeatedly pumped approximately τ_t/τ_s times during the interaction time τ_t. This leads to the minimum value for ω,

$$\frac{\mu^2 E^2}{\hbar^2\omega^2}\frac{\tau_t}{\tau_s} < 1 . \tag{5}$$

Using Eqs. (2) and (4), this gives the same laser power requirement

$$E^2 > \hbar/(\alpha\tau_t)$$

as for the two-step pumping. Therefore, two schemes are equally efficient, provided that the molecule has an excited state with sufficiently large transition moment. A typical spontaneous lifetime of an allowed excited state in the optical region is in the order of 10 ns. A molecule with thermal energy travels only 10 μm during this time. In most of the experimental situations τ_t is longer than τ_s and the stimulated Raman pumping is a better scheme.

When the laser intensity is sufficiently strong for the two-step pumping, the initial population in level 1 in Fig. 1 is equally shared by all three levels during the interaction. After the molecule passes through the interaction region, the population in level 3 is distributed among various vibrational levels in the ground state. The amount increases further when the interaction time is longer than the spontaneous lifetime. For the Raman pumping, the population is shared only by levels 1 and 2. Their populations do not change essentially after the interaction with lasers. This simplifies the analysis of experiments compared to the two-step pumping, where many other levels are also populated by pumping. In an actual application, one may use a mixed scheme by choosing laser frequencies very close to the resonance. The best operation condition depends on the characteristics of available electronic states, the fraction of molecules that may be populated to undesirable levels and also on the angular resolution of the selectively pumped molecular beam. The last factor is related to the resonance width of the pumping. The Raman pumping is usually sharper for a given transition moment and laser intensity. Therefore, a better control on the laser frequency is necessary. In the next section we discuss in detail the characteristics of two-photon pumping by using a simplified formulation.

II. THEORETICAL EVALUATION

We consider a three-level molecule as shown in Fig. 1. Two lasers are assumed to cross perpendicularly with the molecular beam. This configuration has the maximum pumping efficiency because the Doppler shift is canceled. For the velocity selective pumping, one may use angled or parallel configuration.[29–31] The response in this case can be derived from the result given in this section. The temporal evolution of this three-level molecule is described by the following density matrix equation:

$$i\hbar\frac{d\rho}{dt} = [H,\rho] - \frac{i\hbar}{2}[\Gamma,\rho]_+ ,$$

where

$$H = \begin{bmatrix} 0 & 0 & \mu_{13}E \\ 0 & \hbar\omega_{12} & \mu_{23}E \\ \mu_{13}E & \mu_{23}E & \hbar\omega_{13} \end{bmatrix}$$

and $\Gamma_{33}=\gamma_s$, else $\Gamma_{ij}=0$, where γ_s is the spontaneous decay rate from level 3.

The molecule enters the interaction area with the initial condition $\rho_{11}=1$. Quantities we need to calculate are ρ_{22} and ρ_{33} at the exit of the interaction area. To obtain the number of vibrationally excited molecules, they are integrated over the molecular path and velocity. The result depends on the laser-beam pattern at the crossing, the interaction time, and traveling angle of the molecule. We simplify the calculation by assuming that the effect of the interaction time is represented by a relaxation rate $\gamma_i = 1/\tau_i$, where τ_i is the average interaction time. The effect of spatial and temporal inhomogeneity of the laser may be also taken into account by introducing an off-diagonal relaxation rate γ_c corresponding to γ_i. Its inverse $1/\gamma_c$ is the coherent interaction time of the laser with the molecule. The problem is then reduced to solve the steady-state response of the following equations:

$$\begin{aligned}
\dot{\rho}_{11} &= ix_p^*\rho_{31} - ix_p\rho_{13} + \delta_1\gamma_s\rho_{33} - \gamma_i(\rho_{11}-\rho_{11}^{(0)}) , \\
\dot{\rho}_{22} &= ix_s^*\rho_{32} - ix_s\rho_{23} + \delta_2\gamma_s\rho_{33} - \gamma_i\rho_{22} , \\
\dot{\rho}_{33} &= ix_p\rho_{13} - ix_p^*\rho_{31} + ix_s\rho_{23} - ix_s^*\rho_{32} - (\gamma_s+\gamma_i)\rho_{33} , \\
\dot{\rho}_{12} &= ix_p^*\rho_{32} - ix_s\rho_{13} + (i\omega_2 - i\omega_p + i\omega_s - \gamma_c)\rho_{12} , \\
\dot{\rho}_{13} &= ix_p^*(\rho_{33}-\rho_{11}) - ix_s^*\rho_{12} \\
&\quad + \left[i\omega_3 - i\omega_p - \gamma_c - \frac{\gamma_s}{2} \right]\rho_{13} , \\
\dot{\rho}_{23} &= ix_s^*(\rho_{33}-\rho_{22}) - ix_p^*\rho_{21} \\
&\quad + \left[i\omega_3 - i\omega_2 - i\omega_s - \gamma_c - \frac{\gamma_s}{2} \right]\rho_{23} ,
\end{aligned} \tag{6}$$

where $x_p=(\mu_{13}E_p)/\hbar$ and $x_s=(\mu_{23}E_s)/\hbar$ are Rabi frequencies, and ω_p and ω_s are frequency mismatches of transitions $1\rightarrow3$ and $3\rightarrow2$, respectively. In the above equations the laser field is expressed by

$$E=(E_p e^{-i(\omega_{13}+\omega_p)t}+E_s e^{-i(\omega_{23}+\omega_s)t})+\text{c.c.}$$

where $\omega_{23}=\omega_{13}-\omega_{12}$. Coefficients δ_1 and δ_2 are fractions of molecules which decay from level 3 to levels 1 and 2 by spontaneous emission, respectively. $\rho_{11}^{(0)}$ is the number of molecules in level 1 per unit time entering the interaction area. The solution of Eqs. (6) describes the behavior of molecules with same resonance frequency. When the molecular beam and laser cross perpendicularly and the solid angle of excitation is limited by the angular spread of molecules, it is equal to the response by entire molecular beam after the interaction. When two beams cross at an angle other than 90°, or when the angle of excitation is limited by the shape of the laser beam, it describes the behavior of molecules with particular transverse velocity. To obtain the response of entire beam, the solution has to be integrated over velocity.

The population in level 2 after the interaction relative to the initial population in level 1 is

$$I_2=(\rho_{22}+\delta_2\rho_{33})/\rho_{11}^{(0)} \tag{7}$$

and the relative population which goes to levels other than 1 and 2 are

$$I_n=(1-\delta_1-\delta_2)(\gamma_s/\gamma_i+1)\rho_{33}/\rho_{11}^{(0)}\ . \tag{8}$$

Equations (6) with $d/dt=0$ are linear arithmetic equations, and can be solved easily. We show in Fig. 2 typical resonance curves of I_2 as a function of ω_s and ω_p. A peak always runs along Raman resonance $\omega_p=\omega_s$. This is understood by considering that I_2 decreases with frequency mismatch ω by ω^{-2} only along this line and by ω^{-4} in other regions. In addition, the peak due to spontaneous population from level 3 appears along $\omega_p=0$. This effect is exaggerated in the figure by allocating 10% of the spontaneous decay to level 2. When $\gamma_s<\gamma_i$ and $|x_s|^2\approx|x_p|^2$ [Fig. 2(a)], or when the laser intensity is weak, the maximum $I_2^{\max}$ is at the origin. Therefore, the two-step pumping is more efficient than the Raman pumping. When $\gamma_s>\gamma_i$ and $|x_p|^2$ is sufficiently intense to populate level 3 [Fig. 2(b)], I_2 takes the maximum value at finite ω_p and ω_s. If the intensities of the two lasers are fairly different, $|x_p|^2=|x_s|^2$, the Raman peak is twisted around the origin. The direction of the twist is that I_2 becomes double peaked as a function of the frequency of the weaker field as shown in Fig. 2(b). This doublet is the well-known ac Stark splitting caused by the stronger field. In such a case, the maximum is at finite ω_s and ω_p and their values are different.

We show the summary of the calculation over the intensity range $|x|^2$ of $0.001\gamma_i^2$ to $1000\gamma_i^2$ and the spontaneous decay rate γ_s of $0.001\gamma_i$ to $1000\gamma_i$ in the following figures, where frequency is normalized by γ_i. This applies when the result is compared for the same experimental configuration and molecular velocity. The laser-power dependence of many quantities shows two characteristic patterns depending on the magnitude of γ_s relative

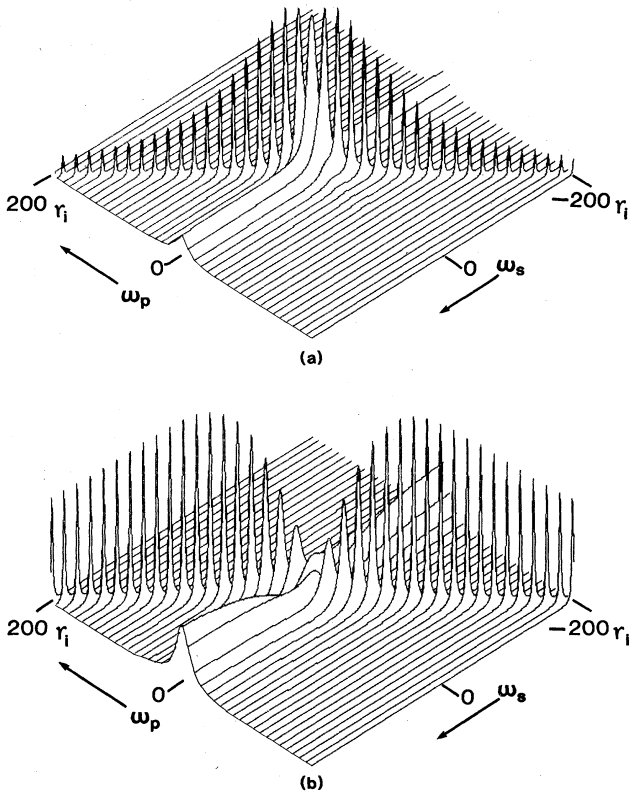

FIG. 2. Relative population in level 2, I_2, as a function of ω_p and ω_s. (a) When the spontaneous lifetime is long, $\gamma_s=0.1\gamma_i$ and $|x_s|^2=|x_p|^2=30\gamma_i^2$. (b) When the spontaneous lifetime is short and the intensity of two lasers is different, $\gamma_s=10\gamma_i$, $|x_s|^2=400\gamma_i^2$, and $|x_p|^2=10\gamma_i^2$. Other parameters are the same for both (a) and (b). $\delta_1=\delta_2=0.1$, $\gamma_c=\gamma_i$.

to γ_i. When $\gamma_s<\gamma_i$, the result is almost identical for the same $|x_s|^2$ and $|x_p|^2$ regardless of γ_s. Since all three are proportional to μ^2, this means that the same pumping efficiency is obtained if the laser intensity is scaled with the spontaneous lifetime. When $\gamma_s>\gamma_i$, the result is similar if $|x_s|^2$ and $|x_p|^2$ are scaled with γ_s. Therefore, the pumping efficiency remains constant for the same laser power, even when the intermediate state with larger transition moment is used. This is because the increase in the spontaneous width pushes the peak frequency to larger value, thus reducing the Raman efficiency.

Figure 3 shows the maximum value of the relative population in level 2, $I_2^{\max}$ for $\gamma_s=0.1\gamma_i$ as a function of laser intensities. It approaches the limiting value of $\frac{1}{2}$, when both $|x_p|^2$ and $|x_s|^2$ exceed γ_i^2. For smaller $|x_p|^2$, $I_2^{\max}$ decreases linearly. The situation is similar for $|x_s|^2$, except that $I_2^{\max}$ is finite even at zero field, because the spontaneous emission from level 3 populates level 2. The curve is almost identical for any value of γ_s smaller than γ_i. When $\gamma_s>\gamma_i$, curves coincide with those in Fig. 3 if $|x_s|^2$ and $|x_p|^2$ are replaced by $|x_s|^2(\gamma_i/\gamma_s)$ and $|x_p|^2(\gamma_i/\gamma_s)$, respectively.

The operation at the maximum pumping efficiency does not give the best discrimination of level 2 from other excited levels. Figure 4 shows the ratio $I_n/I_2^{\max}$ for the

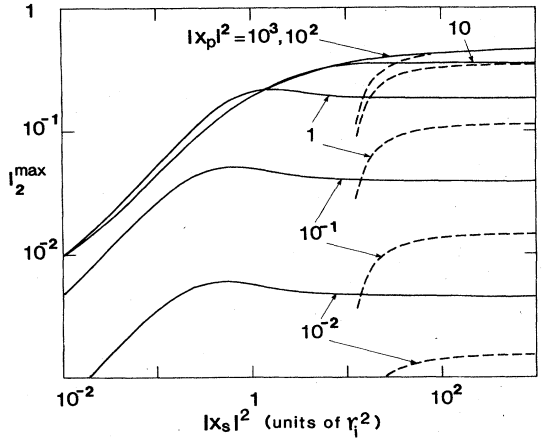

FIG. 3. Maximum relative population in level 2, I_2^{max}, as a function of $|x_s|^2$ (solid lines). Dashed lines are the maximum of I_2 with the restriction $I_n/I_2<0.1$. Other parameters are $\gamma_s=0.1\gamma_i$, $\gamma_c=\gamma_i$, $\delta_1=\delta_2=0.01$. $|x_p|^2$ is in units of γ_i^2.

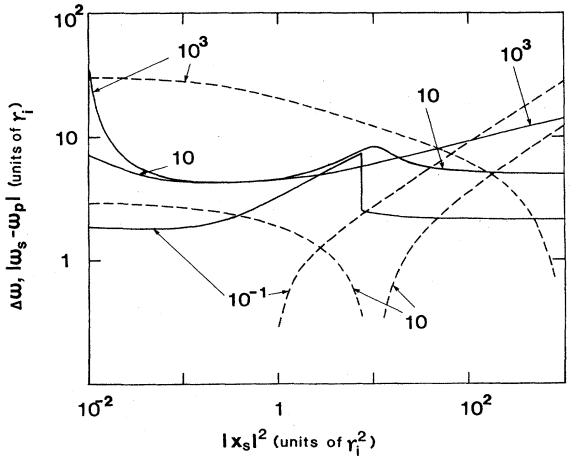

FIG. 5. Full half-width of the population in level 2 measured along $\omega_p=$const (solid lines) and the difference $|\omega_s-\omega_p|$ (dashed lines) at I_2^{max}. Parameters are the same as in Fig. 3. Numbers in the figure are $|x_p|^2$ in units of γ_i^2.

same parameter as in Fig. 3. Curves for other values of γ_s are obtained by the same scaling discussed above for I_2^{max}. I_n/I_2^{max} is always larger than 1 for $|x_s|^2<\gamma_i^2$. It decreases with $|x_s|^2$ to some point, and then flattens beyond that intensity. Its minimum value is estimated from the transition rate at large ω. I_n is populated mostly through the single-photon transition from level 1 to 3. The transition rate is given from the second-order perturbation solution of Eqs. (6) as

$$4|x_p|^2/\omega_p^2 .$$

The Raman transition rate is also obtained by the same method as

$$|x_p|^2|x_s|^2/(\omega_p^2\gamma_i^2) .$$

Therefore, the ratio is

$$I_n/I_2\sim 4\gamma_i^2/|x_s|^2 \tag{9}$$

which depends only on $|x_s|^2$ and γ_i. The laser needs higher intensity if the total population in unwanted levels is kept below the population in level 2. In Fig. 3 the maximum I_2 with the additional restriction of $I_n/I_2=0.1$ is shown by broken lines for various values of $|x_p|^2$.

The total number of molecules in level 2 after the interaction is proportional not only to I_2 but also to the solid angle of the molecular beam excited by lasers. Molecules traveling in the perpendicular plane to the laser do not show a Doppler shift. They are pumped simultaneously regardless of their velocity. If they travel at an angle ϑ from the perpendicular plane, the Doppler shift for ω_p and ω_s is $\omega_{13}\vartheta(v/c)$ and $\omega_{23}\vartheta(v/c)$, respectively. The angle of acceptance is obtained by comparing the Doppler width with the resonance width $\Delta\omega$ along the line $\omega_p/\omega_{13}-\omega_s/\omega_{23}=$const,

$$\vartheta_{max}=\frac{c}{v}\frac{\Delta\omega}{\omega_{13}-\omega_{23}} . \tag{10}$$

This depends on the Stokes shift $\omega_{13}-\omega_{23}$ and transition

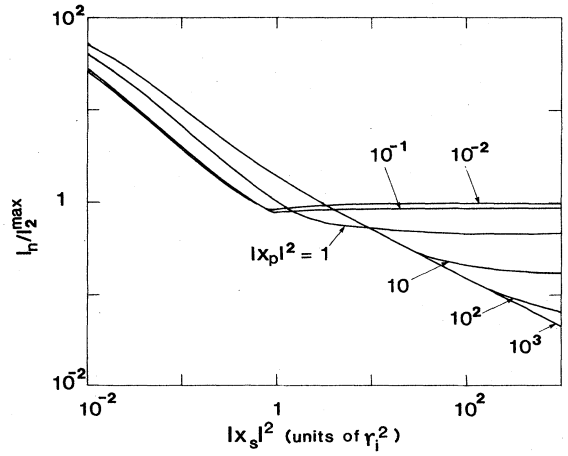

FIG. 4. Population ratio between all levels other than 1, 2, and 3, and level 2, I_n/I_2 at I_2^{max}. Parameters are the same as in Fig. 3. $|x_p|^2$ is in units of γ_i^2.

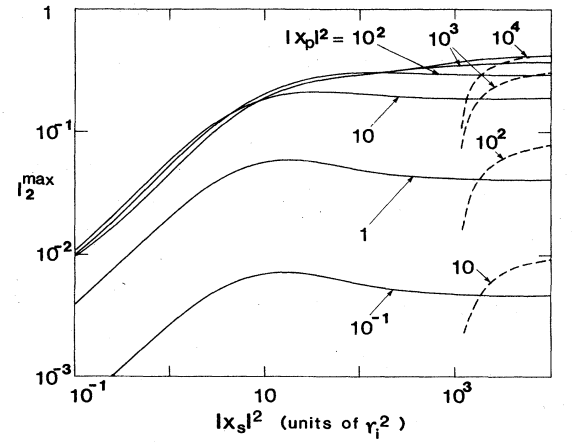

FIG. 6. Maximum relative population in level 2, when the pumping lasers are not perfectly coherent, $\gamma_c=10\gamma_i$. Other parameters are the same as in Fig. 3. $|x_p|^2$ is in units of γ_i^2.

frequencies. Figure 5 shows along $\omega_s = \text{const}$ at $I_2^{\max}$. The width is several times γ_i for some intensity range and increases with $|x_s|^2$ at very high intensity.

The exact Raman condition $\omega_s = \omega_p$ is not always satisfied at the resonance. In Fig. 5 the shift $|\omega_s - \omega_p|$ is shown by broken lines for the same parameters as in Fig. 3. When $|x_s|^2 = |x_p|^2$ this shift disappears. For $|x_s|^2 > |x_p|^2$, the difference is due to the frequency shift of the Raman resonance, while for $|x_s|^2 < |x_p|^2$ it is caused by the ac Stark effect. The shift is smaller than the resonance width if $|x_s|^2$ and $|x_p|^2$ are not extremely different. Actual molecular levels are composed of $2J+1$-fold degenerate magnetic sublevels. Since those sublevels have different transition moments, each sublevel has a different peak frequency and resonance width. As a result, the peak height is reduced and the width is broadened.

Spacial incoherence of lasers also reduces the pumping efficiency. If two lasers are not perfectly overlapping, the Raman peak becomes smaller. However, the two-step peak and the population created by spontaneous emission are not necessarily affected, because they are essentially the sum of two independent processes. When the wavefront is not ideal, the coherent response of molecules is affected. We show in Fig. 6 an example of a calculation with $\gamma_c = 10\gamma_i$. This approximates the case when the laser drives molecules coherently only for $\frac{1}{10}$th of the interaction time. Comparison with Fig. 5 shows that a factor of γ_c/γ_i larger intensity is necessary to obtain the same pumping efficiency.

The above result shows that a vibrational level can be pumped fairly efficiently and also stably by a stimulated Raman process if the lasers are sufficiently intense to saturate respective transitions and their Rabi frequencies are not extremely different. The power required for the pumping may differ in many orders of magnitude for different molecules. For many simple molecules, presently available continuous tunable lasers have sufficient power. For a Na_2 beam, the average velocity is approximately 10^3m/s at the nozzle temperature of 10^3 K. The spontaneous lifetime of $A\,^1\Sigma_g^+$ state is 12 ns.[32,33] Assuming an average transition wavelength of 600 nm and the Frank-Condon factor of 10^{-2} for $2 \rightarrow 3$ transition, the transition moment μ is calculated to be 4.4×10^{-19} esu. For the laser diameter of 1 mm, γ_i is approximately $10^6\ \text{s}^{-1}$. Since this is the case of $\gamma_s > \gamma_i$, the laser power necessary to populate level 2 is γ_s/γ_i times of the power determined by $|x| \sim \gamma_i$. This value is approximately 20 mW. It should be noted, however, that the angle $\vartheta_{\max}$ in Eq. (10) is very small for this configuration. Even for the case of small Stokes shift $\omega_{13} - \omega_{23} = 0.1\omega_{13}$, $\vartheta_{\max}$ is in the order of 10^{-3}. When the nozzle diameter is sufficiently small, one can increase $\vartheta_{\max}$ by focusing the laser to a smaller diameter and by pumping at a proportionally shorter distance from the nozzle. This does not change the angular resolution in the perpendicular plane to the laser, and increases $\vartheta_{\max}$ because it increases γ_i. The power requirement is also reduced proportionally in the region $\gamma_s > \gamma_i$, though it is constant when $\gamma_s < \gamma_i$. Therefore, under usual experimental conditions, the power requirement is determined by the minimum distance between the nozzle and the pumping point, which is determined by molecular interaction in the beam near the nozzle.

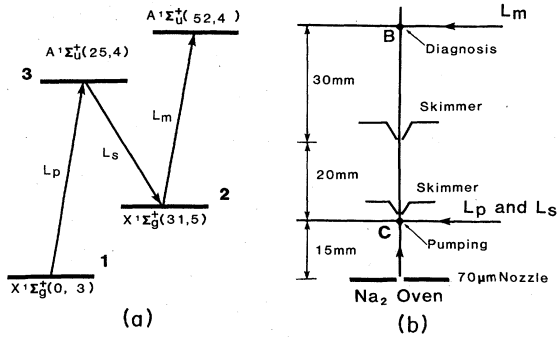

FIG. 7. Energy levels (a) and experimental configuration (b) of the molecular beam and lasers.

III. EXPERIMENT AND DISCUSSIONS

Na_2 has a singlet excited state $A\,^1\Sigma_u^+$, which has a large transition moment with the ground state $X\,^1\Sigma_g^+$, in the frequency range of Rhodamine dye lasers. Equilibrium nuclear distance and rotational constants of two states are fairly different. The energy-level structure of A and X states are simple, and only a few levels of A state are perturbed by other states. Therefore, Na_2 is an ideal molecule for the demonstration of the present technique. Figure 7 shows the geometrical configuration of the molecular beam and energy levels we used for the pumping. Two lasers L_p and L_s pumped the molecule from $v=0, J=3$ to $v=31, J=5$ level, through the intermediate level $v=25, J=4$ of A state. Levels are numbered from 1 to 3 in accordance with Fig. 1. Two pumping lasers were commercial ring dye lasers. L_p was operated with Rhodamine-6G and L_s with LD700 dye. The polarization of L_p was parallel to the molecular beam and the polarization of L_p and L_s was perpendicular to each other. The population in level 2 was monitored by using the third laser L_m. Its frequency was resonant to the transition between level 2 and the $v=52, J=4$ level of the A state. The laser power was approximately 30 mW with a

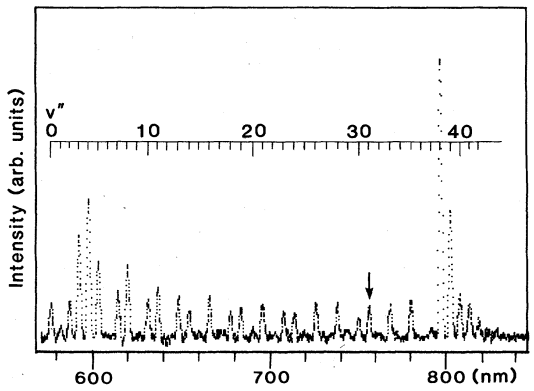

FIG. 8. Fluorescence spectrum from level 1 ($v=25, J=4$ of $A\,^1\Sigma_u^+$). Each line does not resolve R and P transitions. The $v''=0$ peak contains scattering of the excitation laser. The transition from $v'=25$ to $v''=31$ is marked by an arrow.

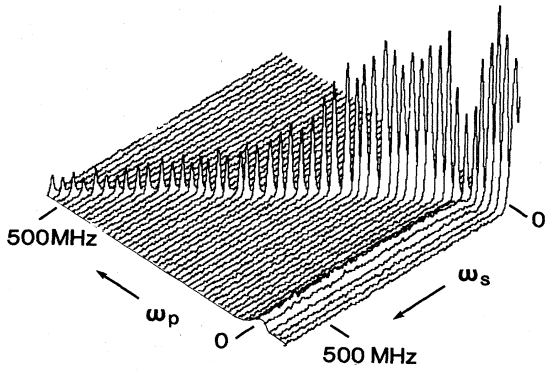

FIG. 9. Fluorescence intensity from $v=52, J=4$ level of $A\,^1\Sigma_g^+$ state as a function of pumping laser frequencies.

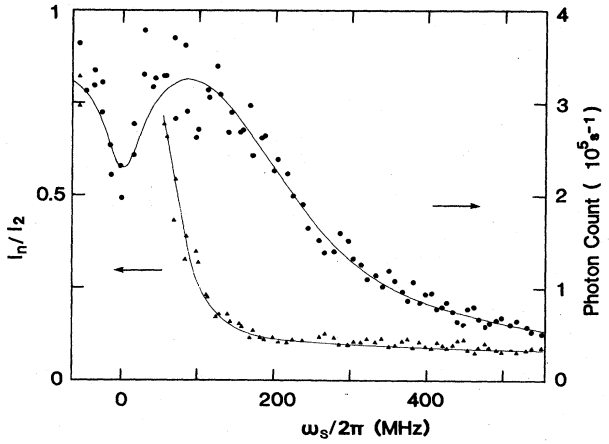

FIG. 10. Fluorescence intensity from level 4 (circles) and I_n/I_2 (triangles) along the Raman peak in Fig. 9. The latter is calculated from the height and width of the spontaneous peak along $\omega_p=0$ in Fig. 9.

diameter of 0.3 mm and was sufficient to saturate this transition. In such a case, the fluorescence intensity from the $v=52$ level is proportional to the number of molecules in level 2 that cross L_m. The laser path was fixed and perpendicular to the molecular beam. No attempt was made to analyze angular or velocity dependence of the pumping efficiency by spacially scanning the monitor laser.

The Na_2 beam was produced from a 70-μm pinhole on 50-μm-thick tantalum foil heated to approximately 1000 K. The beam was seeded by Ar gas with the stagnation pressure of 2 to 4 atm. The pumping lasers were crossed perpendicularly to the Na_2 beam at a distance of 15 mm from the nozzle, just before the first skimmer. The pumping point is marked by C in Fig. 7. Two lasers were aligned into the same pass and focused to form approximately the same diameter of 300 μm at C. The beam passed through the second skimmer and crossed with the monitor laser L_m at B in Fig. 7. The distance between B and the nozzle was 65 mm. The pressure in the nozzle section was 2×10^{-4} Torr and approximately 10^{-6} Torr in the monitor section. Fluorescence emitted at B was collected by two spherical mirrors on an end surface of an optical fiber bundle and detected by a photomultiplier at the other end of the fiber placed outside the vacuum chamber. It was processed by a standard photon counting apparatus.

The pumping point C was determined in the following way. Part of L_p was directed to B simultaneously to excite level 2 at C. Fluorescence induced by L_p at B decreased when the molecule was pumped out from level 1 at C. This change was the largest when C was close to the first skimmer and decreased rapidly when it approached the nozzle. This shows that considerable collisions had taken place even at a distance several millimeters downstream of the nozzle. The ratio of the fluorescence intensity with and without the pumping was approximately 2:1. Figure 8 shows a low-resolution fluorescence spectrum of Na_2, when it was pumped from level 1 to level 3. Each line is the sum of P and R transitions from the same vibrational quantum number. Level 2 was selected from this spectrum. Its branching ratio was 9.7×10^{-3} and was typical among allowed transitions.

Figure 9 shows the population of level 2 as a function of laser frequencies ω_p and ω_s. In the figure, ω_s was repeatedly scanned in a triangular way with a peak-to-peak amplitude of 880 MHz around $\omega_s=0$. Its period was 4.8 s. L_p was scanned slowly in one direction covering 780 MHz in 4 min. Since the scanning of L_s showed hysteresis, the figure shows the spectrum with increasing scanning direction. The laser power at C was 80 mW for L_p and 300 mW for L_s. The intensity peak ran along the Raman resonance as expected from the previous discussion. The photon count at the maximum point was 3.3×10^5 s^{-1}. Considering the quantum efficiency of the photomultipler of 0.1 and the collection efficiency of the optical system of 0.1, this corresponds to the flux of approxiately 3×10^7 s^{-1}. The number of molecules actually excited to level 2 was considerably larger, because L_m did not cover the solid angle of the excitation at C. The relative population I_2 defined in Eq. (7) is estimated from the height of the spontaneous population along $\omega_p=0$. The photon count of the spontaneous population in Fig. 9 was 2.6×10^4 s^{-1}. Combining with the branching ratio of 9.7×10^{-3}, the observed $I_2^{\max}$ is approximately 0.13. Spectral width of the spontaneous population in Fig. 8 is 36 MHz. It is expected to show Lorentzian line shape. This enables us to estimate I_n at large ω_s. In Fig. 10 we plot I_2 and I_n/I_2 along the Raman peak as a function of ω_s. I_2 has the maximum at $\omega_s/2\pi=100$ MHz and decreases gradually with ω_s. The ratio I_n/I_2 is 0.35 at the maximum and approaches 0.08 for large ω_s. Figure 11 shows the full half-width of the Raman resonance. The resonance width is 18 MHz at the maximum of I_2. It decreases with increasing ω_s and also at $\omega_s\sim0$. The latter is not expected from the theory in the preceding section. The present experimental condition corresponds approximately to $\gamma_s=25\gamma_i$, $|x_s|^2=160$, and $|x_p|^2=10$, assuming the average transition moment of 2.2×10^{-19} esu. The numerical analysis predicts $I_2^{\max}=0.4$, $I_n/I_2=0.4$, and the resonance width of 3 MHz at the maximum of I_2 for $\gamma_c=\gamma_i$. The discrepancy on I_2 and the width can be attributed to the spacial and temporal coherence of the

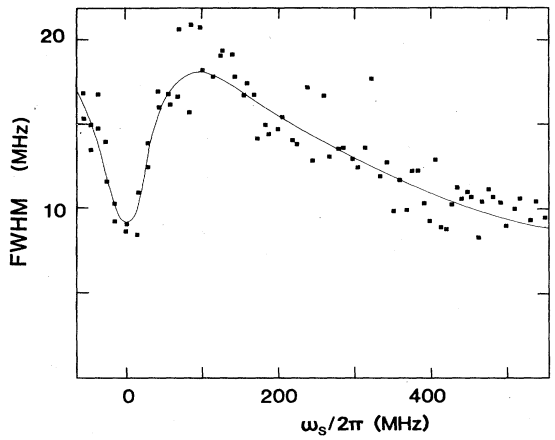

FIG. 11. Full half-width of the Raman resonance as a function of ω_s.

pumping lasers. The resonance width increases nearly proportional to γ_c/γ_i. Spatial misalignment of two pumping lasers decreases the population I_2. The height of the Raman peak in Fig. 9 shows random variation with frequency. This is partly due to the temporal fluctuation of the molecular beam, but is mostly affected by the pointing instability of pumping lasers. The latter is rather difficult to eliminate for a laser with small pumping volume as dye lasers.

We have demonstrated that stimulated Raman pumping by continuous tunable dye lasers can produce a sufficient number of selectively excited molecules for collision study in molecular-beam experiments. The above result shows, however, that it is not easy to obtain a completely uniform excited molecular beam without sacrificing available laser power and beam intensity. Therefore, for an actual application it is more advantageous to analyze beam characteristics after it is pumped rather than to try to generate a prescribed beam, which can be done by the laser-induced fluorescence using an independent monitor laser.

ACKNOWLEDGMENT

This work was supported by a Grant-in-Aid for Fusion Research from the Ministry of Education, Science and Culture, Japan.

[1]A. Schultz, H. W. Cruse, and R.N. Zare, J. Chem. Phys. **57**, 1354 (1972).
[2]J. L. Kinsey, Ann. Rev. Phys. Chem. **28**, 349 (1977).
[3]J. A. Irvin and P. J. Dagdigian, J. Chem. Phys. **74**, 6178 (1981).
[4]M. G. Prisant, C. T. Rettner, and R. N. Zare, J. Chem. Phys. **75**, 2222 (1981).
[5]C. T. Rettner and R. N. Zare, J. Chem. Phys. **75**, 3636 (1981); **77**, 2416 (1982).
[6]J. W. Cox and P. J. Dagdigian, J. Phys. Chem. **86**, 3738 (1982).
[7]H. J. Yuh and P. J. Dagdigian, J. Chem. Phys. **81**, 2375 (1984).
[8]C. Crepin, J. L. Picque, G. Rahmat, J. Verges, R. Vetter, F. X. Gadea, M. Pelissier, F. Spiegelmann, and J. P. Malrieu, Chem. Phys. Lett. **110**, 395 (1984).
[9]K. Bergmann, R. Engelhardt, U. Hefter, P. Hering, and J. Witt, Phys. Rev. Lett. **40**, 1446 (1978).
[10]K. Bergmann, U. Hefter, and J. Witt, J. Chem. Phys. **72**, 4777 (1980).
[11]J. A. Serri, A. Morales, W. Moskowitz, D. E. Pritchard, C. H. Becker, and J. L. Kinsey, J. Chem. Phys. **72**, 6304 (1980).
[12]K. Bergmann, W. Muller, W. Meyer, and R. Schinke, Phys. Rev. A **26**, 1283 (1982).
[13]P. L. Jones, E. Gottwald, U. Hefter, and K. Bergmann, J. Chem. Phys. **78**, 3838 (1983).
[14]W. P. Moskowitz, B. Stewart, R. M. Bilotta, J. L. Kinsey, and D. E. Pritchard, J. Chem. Phys. **80**, 5496 (1984).
[15]T. J. Odiorne, P. R. Brooks, and J. V. V. Kasper, J. Chem. Phys. **55**, 1980 (1971).
[16]J. G. Pruett and R. N. Zare, J. Chem. Phys. **64**, 1774 (1976).
[17]Z. Karny and R. N. Zare, J. Chem. Phys. **68**, 3360 (1978); **69**, 5199 (1978).
[18]H. H. Dispert, M. W. Geis, and P. R. Brooks, J. Chem. Phys. **70**, 5317 (1979).
[19]A. Gupta, D. S. Perry, and R. N. Zare, J. Chem. Phys. **72**, 6237 (1980); **72**, 6250 (1980).
[20]A. Torres-Filho and J. G. Pruett, J. Chem. Phys. **72**, 6736 (1980); **77**, 740 (1982).
[21]C. K. Man and R. C. Estler, J. Chem. Phys. **75**, 2779 (1981).
[22]A. Altkorn, F. E. Bartoszek, J. Dehaven, G. Hancock, D. S. Peny, and R. N. Zare, Chem. Phys. Lett. **98**, 212 (1983).
[23]A. E. DePristo, H. Rabitz, and R. B. Miles, J. Chem. Phys. **73**, 4798 (1980).
[24]D. E. Reisner, R. W. Field, and D. H. Katayama, J. Chem. Phys. **75**, 2056 (1981).
[25]S. V. Amel'kin and A. N. Oraevskii, Izv. Akad. Nauk SSSR, Ser. Fiz. **45**, 1007 (1981).
[26]D. E. Reisner, P. H. Vaccaro, C. Kittrell, R. W. Field, J. L. Kinsey, and H. L. Dai, J. Chem. Phys. **77**, 573 (1982).
[27]F. Shimizu, K. Shimizu, and H. Takuma, Chem. Phys. Lett. **102**, 375 (1983).
[28]P. L. Jones, U. Gaubatz, U. Hefter, K. Bergmann, and B. Wellegehausen, Appl. Phys. Lett. **42**, 222 (1983).
[29]K. Bergmann, U. Hefter, and P. Hering, Chem. Phys. **32**, 329 (1978).
[30]E. J. Murphy, J. H. Brophy, and J. L. Kinsey, J. Chem. Phys. **74**, 331 (1981).
[31]J. A. Serri, J. L. Kinsey, and D. E. Pritchard, J. Chem. Phys. **75**, 663 (1981).
[32]T. W. Ducas, M. Littman, M. L. Zimmerman, and D. Kleppner, J. Chem. Phys. **65**, 842 (1976).
[33]G. Baumgartner, H. Kornmeier, and W. Preuss, Chem. Phys. Lett. **107**, 13 (1984).